Redetermination of the valley-orbit (chemical) splitting of the 1s ground state of group-V donors in silicon

A. J. Mayur, M. Dean Sciacca, A. K. Ramdas, and S. Rodriguez
Department of Physics, Purdue University, West Lafayette, Indiana 47907
(Received 5 February 1993)

The sixfold degeneracy of the $1s(A_1+E+T_2)$ ground state of substitutional group-V donors in Si, originating from the six Δ conduction-band minima, is lifted by the valley-orbit (chemical) splitting, with $1s(E)$ and $1s(T_2)$ remaining close to the effective-mass position and $1s(A_1)$ depressed significantly. The binding energies of $1s(A_1)$, $1s(E)$, and $1s(T_2)$ are accessible to an experimental determination through the observation of the $1s(A_1), 1s(E), 1s(T_2) \rightarrow np_0, np_\pm$ transitions in the Lyman spectrum of the neutral donors, where the p_0 and $p_\pm$ levels are accurately described in the effective-mass theory. We have remeasured the excitation spectrum of Si(P, As, Sb, or Bi) in the temperature range 1.8–100 K under high resolution and signal-to-noise ratio; while only the $1s(A_1) \rightarrow np_0$, $np_\pm$ transitions are observed at the lowest temperature, the $1s(E), 1s(T_2) \rightarrow np_0, np_\pm$ transitions appear on thermally populating $1s(E)$ and $1s(T_2)$. In this manner we have recorded the $1s(E), 1s(T_2) \rightarrow 2p_0, 2p_\pm$ transitions in Si(P, As, and Sb) at optimum temperatures in the range 20–80 K. In Si(Sb), the transitions which originate from $1s(T_2)$ are doublets but not those from $1s(E)$. This feature arises from the inclusion of the spin-orbit interaction which lifts the sixfold degeneracy of $1s(T_2{:}\Gamma_5)$ resolving it into a doublet $1s(T_2{:}\Gamma_7)$ and a quadruplet $1s(T_2{:}\Gamma_8)$; the latter has a smaller binding energy implying a positive value for the spin-orbit coupling parameter. The corresponding observations in Si(Bi) reported here show the spin-orbit splitting of $1s(T_2{:}\Gamma_5)$ in Bi and yield a binding energy of 30.1 meV for $1s(E{:}\Gamma_8)$.

I. INTRODUCTION

In the effective-mass theory (EMT) of substitutional group-V donors in the elemental semiconductors Si or Ge, the orbital wave functions of the donor-bound electron are the hydrogenic envelope functions modulated by the Bloch functions of the energetically equivalent conduction-band (CB) minima.[1–3] The theory thus automatically endows each eigenstate of the donor electron with a multivalley degeneracy, six for Si and four for Ge in view of their $\langle 100 \rangle, \Delta$, and $\langle 111 \rangle, L$, CB minima, respectively. According to this model, all the group-V donors have the same ionization energy E_I for a given host, independent of the chemical nature of the impurity. This is contrary to the experimental facts: in Si, for example, E_I for the substitutional group-V donors ranges from 42.74 meV for Sb to 70.98 meV for Bi whereas EMT yields 31.27 meV.[4] While the values of E_I are indeed very small, consistent with the hydrogenic model, the larger values found experimentally represent a significant departure from EMT. On the basis of the hydrogenic model one expects a Lyman spectrum arising from the $1s \rightarrow np$ transitions in the infrared for neutral donors; such spectra are in fact observed. However, they exhibit a striking feature: while all the group-V donors have excitation lines with the same spacings between corresponding lines with similar relative intensities, the entire spectrum of one is displaced in energy with respect to that of the others. The identity of the spacings is explained by recognizing that the p states of all the donors are accurately predicted by EMT since the p-state wave functions have negligible amplitude at the donor site and any departure from the screened Coulomb potential in the immediate vicinity of the donor site has no significant effect on their binding energies. In contrast, the s states—in particular the $1s$ ground state—with large amplitudes at the donor site experience *chemical shifts* dependent on the chemical species of the donor, thus accounting for the shift of the Lyman spectrum of a given donor with respect to that of another. In Fig. 1 we show schematically the relevant energy levels in EMT and those for a typical substitutional group-V donor.

The separation between $2p_0$ and $2p_\pm$ is a consequence of the effective-mass anisotropy; it is fully accounted for in EMT incorporating a CB with axial symmetry and the associated effective-mass anisotropy.[1] Since the eigenfunctions of the electronic states must conform to the tetrahedral (T_d) site symmetry of the donor, they are classified according to its irreducible representations, as shown on the right-hand side of Fig. 1.[5] Thus the $2p_0$ and $2p_\pm$ states belong to A_1+E+T_2 and $2T_1+2T_2$, respectively. To the extent the spherically symmetric Coulomb potential adequately represents the physical situation, the eigenstates belonging to different irreducible representations are accidentally degenerate as in the case of A_1, E, and T_2 of $2p_0$ and the two T_1's and T_2's of $2p_\pm$. In contrast, the departure from the spherically symmetric Coulomb potential in the immediate vicinity of the donor site lifts the sixfold degeneracy of $1s(A_1+E+T_2)$, resolving it into $1s(A_1)$, $1s(E)$, and $1s(T_2)$. This decomposition is referred to in the literature as *valley-orbit* or *chemical* splitting. The linear combinations of the wave functions are such that $1s(A_1)$ departs from the EMT value significantly whereas $1s(E)$

0163-1829/93/48(15)/10893(6)/$06.00

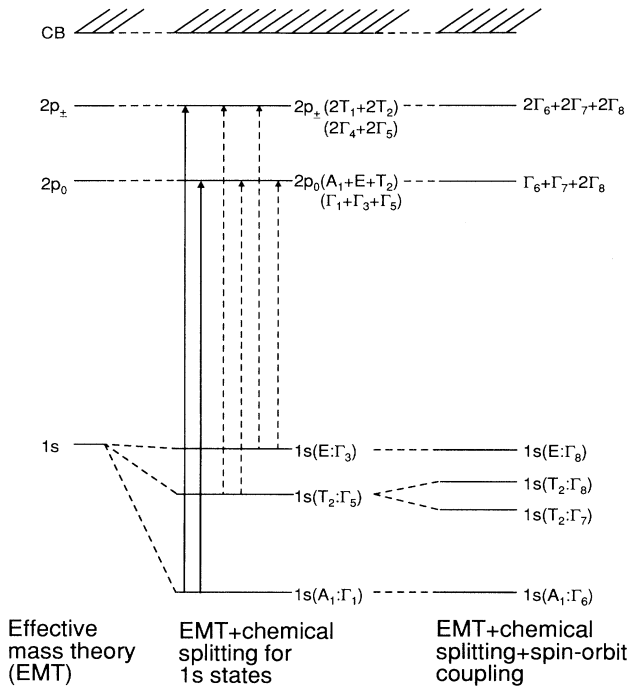

FIG. 1. Energy-level scheme (not to scale) of group-V donors in Si. The letters next to the levels indicate the irreducible representations of T_d, labeled according to the notation used in Ramdas and Rodriguez (Ref. 3) as well as that in Koster *et al.* (Ref. 5).

and $1s(T_2)$ remain close to it.[1-3] In this picture the differences in E_I for the different group-V donors arise from the increased binding energy of $1s(A_1)$, the increase being *chemical species dependent.* Introduction of the spin of the donor electron requires a symmetry classification based on the double valued representations of $\bar{T}_d$, viz., the doublets Γ_6 and Γ_7 and the quadruplet Γ_8 in Koster *et al.*[5] The energy levels shown in Fig. 1 are also labeled accordingly and display the spin-orbit splitting of the $1s(T_2{:}\Gamma_5)$ into $1s(T_2{:}\Gamma_7)$ and $1s(T_2{:}\Gamma_8)$. Note that for $\bar{T}_d$, $\Gamma_1\times\Gamma_6=\Gamma_6$ and $\Gamma_3\times\Gamma_6=\Gamma_8$; hence $1s(A_1{:}\Gamma_1)$ and $1s(E{:}\Gamma_3)$ become a doublet and a quadruplet, respectively. At the lowest temperature only $1s(A_1)$ is occupied by the donor electron and hence one observes the $1s(A_1)\rightarrow np_0$, $np_\pm$ transitions in absorption. The spacings of the excitation lines are consequently the same for all the group-V impurities but the spectra are displaced with respect to one another by the differences in the binding energies of $1s(A_1)$.

From Fig. 1 it can be seen that $1s(E), 1s(T_2) \rightarrow np_0, np_\pm$ transitions can be observed by *thermally populating* the effective-mass-like $1s(E)$ and $1s(T_2)$ states. The temperature at which such transitions can be observed depends on the extent to which $1s(A_1)$ is depressed below $1s(E)$ and $1s(T_2)$. One must clearly perform such experiments at temperatures sufficiently high to populate the upper $1s$ levels but low enough to avoid thermal ionization as well as line broadening. For the earlier work along these lines on group-V donors in Si and Ge we refer the reader to Refs. 6–9.

The present work has been motivated by the significant strides in instrumentation in the past 25 years, viz. (1) the increased figure of merit of the detector (D^*), D^* (composite Si bolometer) $\sim 2\times10^{12}$ cm $Hz^{1/2}/W$ (Ref. 10) as compared to D^* (thermocouple) $\sim 10^9$ cm $Hz^{1/2}/W$; (2) a maximum resolution of 0.0026 cm^{-1} accessible with a BOMEM DA.3 Fourier transform spectrometer[11] (FTS) as compared to that of a double-pass grating spectrometer (0.25 cm^{-1}) used in our earlier measurements; (3) the variable temperature cryostat[12] in which one can make measurements at any desired temperature between 1.8 and 300 K as compared to the fixed bath temperatures accessible in a glass cryostat (4.2 K for liquid He, 20 K for liquid H_2, 77 K for liquid N_2, 90 K for liquid O_2, 195 K for dry ice and additional fixed temperatures reached by pumping on the coolant). In addition, the multiple rapid-scanning feature of the FTS, the convenient data acquisition/processing as well as the ease of studying several samples in succession without warming the cryostat, have enabled high quality data to be acquired on a reasonable time scale. An apodized resolution of 0.05–0.5 cm^{-1} was typically adequate in our measurements and the signal-to-noise ratio was improved by coadding each spectrum 50 times.

II. EXPERIMENTAL RESULTS AND DISCUSSION

The Lyman spectrum of Si(P) at liquid-helium temperature in the energy range from 18 to 45 meV shows the well-known $1s(A_1)\rightarrow np_0, np_\pm$ transitions between 34 and 45 meV (Ref. 13) whereas the energy range from 18 to 34 meV is characterized by the absence of any excitation lines. In contrast, excitation lines appear in the lower energy range with increasing intensity as the temperature is increased, as can be seen from Fig. 2; they are due to the $1s(E), 1s(T_2)\rightarrow np_0, np_\pm$ transitions and their increasing intensity with temperature is a consequence of the increasing thermal population of $1s(E)$ and $1s(T_2)$. The ordering of $1s(E)$ and $1s(T_2)$ has been determined by comparing the calculated and experimental intensities of the transitions from these two states to a common excited state[8] and fully confirmed by uniaxial stress measurements which show that the number and positions of the stress-induced components as well as their polarization characteristics are consistent with the ordering in which $1s(E)$ lies above $1s(T_2)$.[9]

Figures 3 and 4 show the excitation spectra of Si(As) and Si(Sb), respectively, in the energy range between 18 and 30 meV. At the lowest temperatures ($T\sim20$ K for As and $T\sim10$ K for Sb) no lines are seen. However, as in the case of Si(P), upon raising the temperature, the $1s(E), 1s(T_2)\rightarrow np_0, np_\pm$ transitions appear with increasing intensity. It is clearly seen that the larger the chemical shift of $1s(A_1)$ from the EMT value, the smaller the thermal population of $1s(E)$ and $1s(T_2)$ and consequently the larger the temperature necessary for the onset of the transitions from $1s(E)$ and $1s(T_2)$. Such transitions are observed only above ~30 K for Si(As) for which

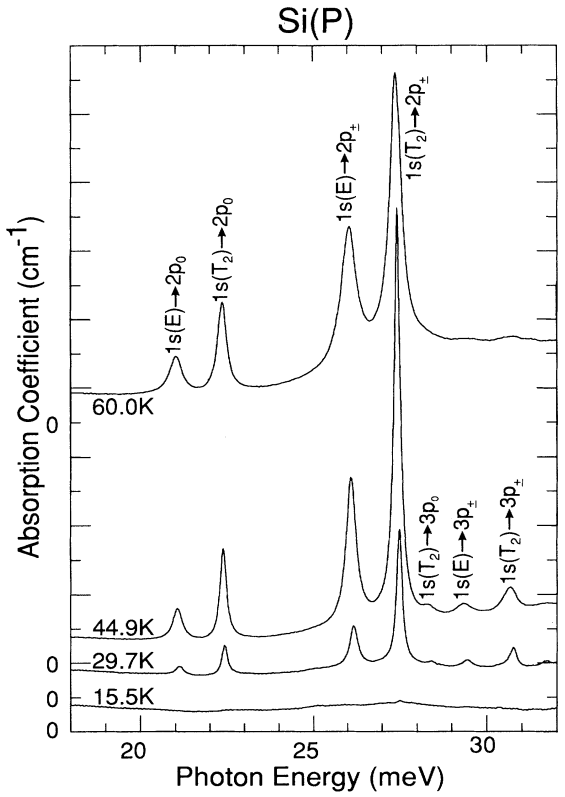

FIG. 2. Excitation spectra of phosphorus donors in silicon at $T=15.5$, 29.7, 44.9, and 60.0 K showing the $1s(E), 1s(T_2) \rightarrow np_0, np_\pm$ transitions, seen as a result of the thermal population of the $1s(E)$ and $1s(T_2)$ levels. Each division of the abscissa corresponds to 2.5 cm^{-1} and the spectra have been displaced vertically for ease of comparison, the base lines for each spectrum being shown by zeros. The concentration of phosphorus is $\sim 5.2\times 10^{15}$ cm^{-3}.

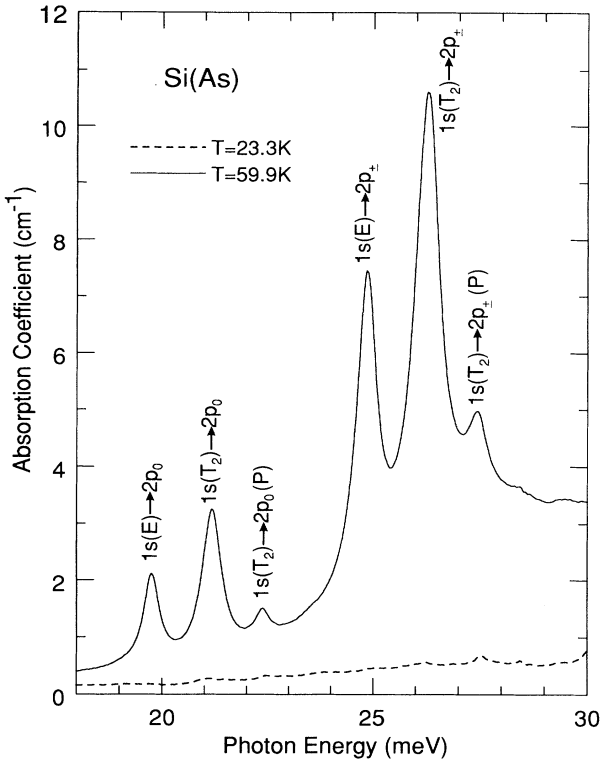

FIG. 3. Excitation spectra of arsenic donors in silicon at 23.3 and 59.9 K showing the $1s(E), 1s(T_2) \rightarrow 2p_0, 2p_\pm$ transitions. The transitions labeled with (P) are due to phosphorus impurity in the sample. The concentration of arsenic donors is $\sim 1.4\times 10^{16}$ cm^{-3}.

$1s(A_1)$ lies ~ 20 meV below $1s(E)$ and $1s(T_2)$ in contrast to Si(Sb) for which they start appearing above ~ 15 K since its $1s(A_1)$ lies only ~ 10 meV below $1s(E)$ and $1s(T_2)$.

An interesting feature in the Si(Sb) spectrum is the doublet structure of all the transitions originating from $1s(T_2)$ (Ref. 9) with the separation between the components decreasing from ~ 0.3 meV at 15 K to ~ 0.2 meV at 60 K. The occurrence of the doublet has been attributed to the spin-orbit interaction $(\hbar/2m^2c^2)(\nabla U \times \mathbf{p})\cdot\mathbf{S}$, which lifts the sixfold degeneracy of $1s(T_2{:}\Gamma_5)$, resolving it into a doublet $1s(T_2{:}\Gamma_7)$ and a quadruplet $1s(T_2{:}\Gamma_8)$.[14] Here U is the potential experienced by the donor electron and $\mathbf{S}$ its spin operator. Noting that $\nabla U \times \mathbf{p}$ is a pseudovector and therefore transforms according to Γ_4, the spin-orbit splitting of $1s(T_2{:}\Gamma_5)$ into $1s(T_2{:}\Gamma_7)$ and $1s(T_2{:}\Gamma_8)$ is described by the effective spin-orbit interaction $\lambda\mathbf{I}\cdot\mathbf{S}$ where

$$\lambda = \frac{\hbar^2}{2m^2c^2}\left\langle \varepsilon_x \left| \frac{\partial U}{\partial x}\frac{\partial}{\partial y} - \frac{\partial U}{\partial y}\frac{\partial}{\partial x} \right| \varepsilon_y \right\rangle . \quad (1)$$

Here ε_x and ε_y are the first two states defined in Eq. (3.50) of Ref. 3 while I_x, I_y, and I_z are the angular momentum matrices defined in Eq. (3.12) of the same reference. The energy separation between the $1s(T_2{:}\Gamma_7)$ and $1s(T_2{:}\Gamma_8)$ sublevels is $3\lambda/2$. We can also calculate the ratio of the intensities of the transitions originating from $1s(T_2{:}\Gamma_8)$ to those arising from $1s(T_2{:}\Gamma_7)$ and terminating in the same np_0 or $np_\pm$ state because their transition probabilities can be expressed in terms of the square amplitude of a single matrix element of the electric dipole operator. This conclusion follows by noting that the transition amplitudes are different from zero only for elements arising from those components of the initial and final states which are associated with one and the same CB minimum. The relative probability amplitudes of the different components of $\Gamma_5\times\Gamma_6=\Gamma_7+\Gamma_8$, thus determined using the Clebsch-Gordan coefficients for the group $\bar{T}_d$, yield a ratio of 2:1 for the intensity of the $1s(T_2{:}\Gamma_8)\rightarrow np_0, np_\pm$ to that of $1s(T_2{:}\Gamma_7) \rightarrow np_0, np_\pm$. This is in excellent agreement with an experimentally measured ratio of 2.0 ± 0.05. We also note that the lower energy component always being stronger is consistent with $1s(T_2{:}\Gamma_8)$ lying above $1s(T_2{:}\Gamma_7)$, i.e., $\lambda > 0$.

The role of thermal population in the $1s(E), 1s(T_2) \rightarrow np_0, np_\pm$ transitions is most dramatically manifested in the case of Si(Bi) where the separation be-

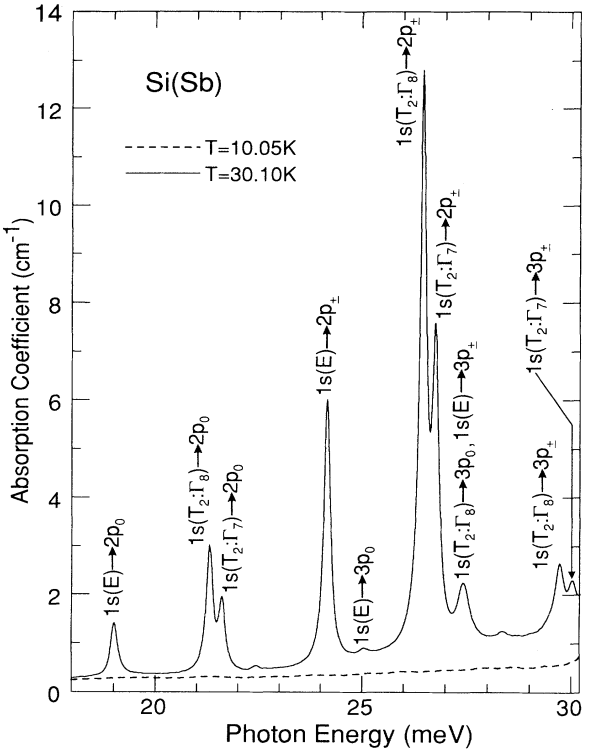

FIG. 4. Excitation spectra of antimony donors in silicon at 10.05 and 30.10 K showing the $1s(E), 1s(T_2) \rightarrow np_0, np_\pm$ transitions. The splitting of the $1s(T_2)$ level due to the residual spin-orbit effect of antimony in silicon is clearly observed. The concentration of antimony donors is $\sim 2.6 \times 10^{15}$ cm^{-3}.

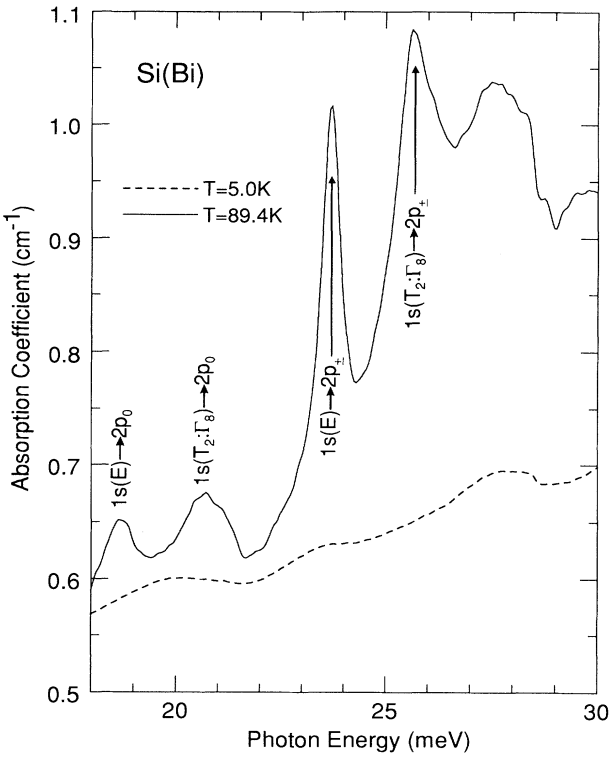

FIG. 5. Excitation spectra of bismuth donors in silicon at 5.0 and 89.4 K showing the $1s(E), 1s(T_2) \rightarrow 2p_0, 2p_\pm$ transitions. The concentration of bismuth donors is $\sim 2 \times 10^{15}$ cm^{-3}.

tween $1s(A_1)$ and $1s(E), 1s(T_2)$ is the largest among the group-V donors, viz. ~39 meV. By thermally populating the latter we have observed for the first time the $1s(E), 1s(T_2) \rightarrow 2p_0, 2p_\pm$ transitions in Si(Bi) at temperatures above 50 K. In Fig. 5 the absorption spectra of a Si(Bi) sample at 5.0 and 89.4 K are displayed in the energy range 18 to 30 meV. Since Bi has a much higher atomic number than that of Sb, it exhibits a much larger spin-orbit splitting of $1s(T_2)$. Krag, Kleiner, and Zeiger[14] reported the spin-orbit split components of the weak $1s(A_1) \rightarrow 1s(T_2)$ transition with a separation of 1 meV between $1s(T_2{:}\Gamma_7)$ and $1s(T_2{:}\Gamma_8)$ at 10 K. They also observed that the transition to the upper $1s(T_2{:}\Gamma_8)$ quadruplet from $1s(A_1{:}\Gamma_6)$ is twice as strong as that to the lower $1s(T_2{:}\Gamma_7)$ doublet. In our measurements, we could not observe these weak $1s(A_1{:}\Gamma_6) \rightarrow 1s(T_2{:}\Gamma_7), 1s(T_2{:}\Gamma_8)$ transitions because the concentration of Bi donors in the sample studied (2×10^{15} cm^{-3}) is significantly smaller than that in the one studied by Krag, Kleiner, and Zeiger ($\sim 10^{16}$ cm^{-3}). However in Fig. 5 we have identified the $1s(E{:}\Gamma_8) \rightarrow 2p_0, 2p_\pm$ and the $1s(T_2{:}\Gamma_8) \rightarrow 2p_0, 2p_\pm$ transitions. We note that the latter are broader than the former and exhibit a high energy asymmetry, consistent with the presence of the weaker $1s(T_2{:}\Gamma_7) \rightarrow 2p_0, 2p_\pm$ transitions. Temperature broadening and a possible decrease in the separation between the spin-orbit split components as in Si(Sb) would preclude a clear resolution of $1s(T_2{:}\Gamma_7) \rightarrow 2p_0, 2p_\pm$ from $1s(T_2{:}\Gamma_8) \rightarrow 2p_0, 2p_\pm$. At 89.4 K, the $1s(T_2{:}\Gamma_8) \rightarrow 2p_0$ and $2p_\pm$ transitions occur at 20.7 and 25.7 meV, respectively. These positions agree with the values of 20.45 and 25.52 meV at 10 K, deduced by subtracting the energy of the $1s(A_1{:}\Gamma_6) \rightarrow 1s(T_2{:}\Gamma_8)$ transition, i.e., 39.09 meV reported by Krag, Kleiner, and Zeiger, from the energies of $1s(A_1{:}\Gamma_6) \rightarrow 2p_0$ and $2p_\pm$ transitions, i.e., 59.54 and 64.61 meV, respectively, measured by Butler, Fisher, and Ramdas.[15] The $1s(E{:}\Gamma_8) \rightarrow 2p_0, 2p_\pm$ transitions identified in Fig. 5 occur at 18.7 and 23.7 meV, respectively, with a separation of 5.0 meV again in excellent agreement with the $(2p_\pm - 2p_0)$ separation of 5.07 meV measured by Butler, Fisher, and Ramdas.[15] A binding energy of 30.1 meV for $1s(E)$ is then obtained by adding the binding energy of $2p_0$ or $2p_\pm$ (Ref. 15) to the transition energy of the $1s(E) \rightarrow 2p_0$ or $1s(E) \rightarrow 2p_\pm$ transition, respectively. We note that $1s(A_1) \rightarrow 1s(E)$ is electric dipole forbidden, but in the presence of the spin-orbit interaction, $1s(A_1{:}\Gamma_6) \rightarrow 1s(E{:}\Gamma_8)$ is allowed although it is much weaker than $1s(A_1{:}\Gamma_6) \rightarrow 1s(T_2{:}\Gamma_7), 1s(T_2{:}\Gamma_8)$ because the latter have T_2 orbital characteristics. Indeed an inspection of the Si(Bi) spectrum displayed in Fig. 1 of Krag, Kleiner, and Zeiger[14] shows a weak but distinct feature at 40.8 meV consistent with its being the

TABLE I. Observed energies of the $1s(E), 1s(T_2) \rightarrow 2p_0, 2p_\pm$ transitions for the various group-V substitutional donors in silicon. The experimental errors in the temperature and energies are ± 0.1 K and ± 0.01 meV, respectively.

Donor	Temperature (K)	Transition energies (meV) $1s(E) \rightarrow 2p_0$	$1s(T_2) \rightarrow 2p_0$	$1s(E) \rightarrow 2p_\pm$	$1s(T_2) \rightarrow 2p_\pm$
P	44.9	21.08	22.41	26.14	27.48
As	59.9	19.75	21.18	24.86	26.29
Sb	30.1	19.02	21.61(Γ_7)	24.16	26.76(Γ_7)
			21.32(Γ_8)		26.46(Γ_8)
Bi	89.4	18.7	(Γ_7)	23.7	(Γ_7)
			20.7(Γ_8)		25.7(Γ_8)
EMT[a]	0	19.76	19.76	24.87	24.87

[a]See Ref. 4.

$1s(A_1{:}\Gamma_6) \rightarrow 1s(E{:}\Gamma_8)$ transition. The binding energy of $1s(E{:}\Gamma_8)$ thus deduced, 30.15 meV, agrees well with 30.1 meV obtained in the present work.

III. SUMMARY

The results of the present investigation are compiled in Table I where the observed energies of the $1s(E), 1s(T_2) \rightarrow 2p_0, 2p_\pm$ transitions for the various group-V donors in silicon and the values calculated from EMT are compared. While there is excellent agreement with the results obtained by us previously for Si(P, As, and Sb),[9] the spectra have been recorded under significantly superior signal-to-noise (S/N) ratio, spectral resolution, and optimum sample temperature. The $1s(E), 1s(T_2) \rightarrow 2p_0, 2p_\pm$ in Si(Bi) are reported here. The binding energy for the upper spin-orbit split $1s(T_2{:}\Gamma_8)$ deduced from our measurements is in agreement with that obtained from the weak $1s(A_1) \rightarrow 1s(T_2{:}\Gamma_8)$ transition observed by Krag, Kleiner, and Zeiger.[14] From the present measurements and the previously unidentified $1s(A_1{:}\Gamma_6) \rightarrow 1s(E{:}\Gamma_8)$ transition of Krag, Kleiner, and Zeiger we conclude that the binding energy of $1s(E{:}\Gamma_8)$ in Si(Bi) is 30.1 meV. During the course of our investigations we have observed a typical decrease of ~ 0.2 meV in the transition energies of $1s(E), 1s(T_2) \rightarrow 2p_0, 2p_\pm$ as the temperature was increased from 20 to 80 K, whereas the transition energy of $1s(A_1) \rightarrow np_0, np_\pm$ increased only by ~ 0.07 meV in going from 2 to 60 K. Hence any intercomparison between donors as well as the comparison of experimental values with those predicted by EMT must take into account this small temperature effect. Again, an accurate measurement of these shifts with temperature was facilitated by the reliable measurement of sample temperature and the excellent S/N ratio of the spectra shown in the figures which represent actual data points without any averaging of the noise except that achieved with coaddition. Another interesting temperature effect is the increase in the linewidths with increasing temperature. We have observed a typical increase of ~ 0.5 meV in the full width at half maximum for the $1s(E), 1s(T_2) \rightarrow 2p_0, 2p_\pm$ transitions between 25 and 80 K and ~ 0.1 meV for the $1s(A_1) \rightarrow np_0, np_\pm$ transitions between 2 and 80 K. A systematic determination of the linewidths and line shifts and their comparison with the theoretical calculations of Barrie and Nishikawa[16] is planned in the future. Finally, the electric dipole forbidden $1s(A_1) \rightarrow 1s(E)$ transitions in group-V donors are allowed in the electronic Raman scattering, thus complementing the infrared absorption data. Such Raman lines have been reported for Si(P, As, and Sb) (Refs. 17 and 18) and their positions are in excellent agreement with those deduced from absorption measurements.

ACKNOWLEDGMENTS

The work reported in this paper was supported by National Science Foundation Grant No. DMR 89-21717.

[1]W. Kohn and J. M. Luttinger, Phys. Rev. **98**, 915 (1955).

[2]W. Kohn, Solid State Physics, edited by F. Seitz and D. Turnbull (Academic, New York, 1957), Vol. 5, p. 257.

[3]A. K. Ramdas and S. Rodriguez, Rep. Prog. Phys. **44**, 1297 (1981).

[4]R. A. Faulkner, Phys. Rev. **184**, 713 (1969).

[5]In the absence of spin the irreducible representations for the donor states with T_d symmetry are denoted by the notation in Ref. 3 as well as that in G. F. Koster, J. O. Dimmock, R. G. Wheeler, and H. Satz, *Properties of the Thirty-two Point Groups* (MIT Press, Cambridge, MA, 1963). Note the irreducible representation A_1, A_2, E, T_1, and T_2 in Ref. 3 correspond to Γ_1, Γ_2, Γ_3, Γ_4, and Γ_5, respectively, in Koster *et al.*

[6]In the case of Group-V donors in Ge, the effective-mass ground state is $1s(A_1+T_2)$, with $1s(A_1)$ showing larger species-dependent binding energies, ranging from 10.32 meV for Sb to 14.18 meV for As. See J. H. Reuszer and P. Fisher, Phys. Rev. **135**, A1125 (1964).

[7]P. Fisher, J. Phys. Chem. Solids **23**, 1346 (1962) showed that the effective-mass ground state of a group-V donor—$1s(T_2)$ for Ge—can be thermally populated and give rise to the $1s(T_2) \rightarrow np_0, np_\pm$ transitions in the Lyman spectrum.

[8]R. L. Aggarwal, Solid State Commun. **2**, 163 (1964). See also F. P. Ottensmeyer, J. C. Giles, and J. W. Bichard, Can. J. Phys. **42**, 1826 (1964).

[9]R. L. Aggarwal and A. K. Ramdas, Phys. Rev. **140**, A1246

(1965).
[10]Infrared Laboratories, Inc., 1808 East 17th Street, Tucson, AZ 85719.
[11]BOMEM, Inc., 450 Avenue, St-Jean Baptiste, Quebec, Canada, G2E 5S5.
[12]Model 10DT Supervaritemp Optical Cryostat, manufactured by Janis Research Company, Inc., 2 Jewel Drive, Wilmington, MA 01887.
[13]C. Jagannath, Z. W. Grabowski, and A. K. Ramdas, Phys. Rev. B **23**, 2082 (1981).
[14]W. E. Krag, W. H. Kleiner, and H. J. Zeiger, *Proceedings of the 10th International Conference on the Physics of Semiconductors, Cambridge, MA, 1970,* edited by S. P. Keller, J. C. Hensel, and F. Stern (USAEC Division of Technical Information Extension, Oak Ridge, TN, 1970), p. 271. See H. J. Zeiger, W. E. Krag, and L. M. Roth (unpublished) and W. E. Krag and H. J. Zeiger, Phys. Rev. Lett. **8**, 485 (1962) where the first observations of the spin-orbit splitting of the $1s(T_2)$ state in Si(Bi) and Si(S) have been reported, respectively. L. M. Roth (unpublished) suggested the spin-orbit origin of such a splitting.
[15]N. R. Butler, P. Fisher, and A. K. Ramdas, Phys. Rev. B **12**, 3200 (1975).
[16]R. Barrie and K. Nishikawa, Can. J. Phys. **41**, 1823 (1963).
[17]G. B. Wright and A. Mooradian, Phys. Rev. Lett. **18**, 608 (1967).
[18]K. Jain, S. Lai, and M. V. Klein, Phys. Rev. B **13**, 5448 (1976).